Development of Mixed Metal Oxides for Thermochemical Hydrogen Production from Solar Water-splitting

A. Le Gal, S. Abanades, G. Flamant

This document appeared in

Detlef Stolten, Thomas Grube (Eds.):
18th World Hydrogen Energy Conference 2010 - WHEC 2010
Parallel Sessions Book 2: Hydrogen Production Technologies – Part 1
Proceedings of the WHEC, May 16.-21. 2010, Essen
Schriften des Forschungszentrums Jülich / Energy & Environment, Vol. 78-2
Institute of Energy Research - Fuel Cells (IEF-3)
Forschungszentrum Jülich GmbH, Zentralbibliothek, Verlag, 2010
ISBN: 978-3-89336-652-1

Development of Mixed Metal Oxides for Thermochemical Hydrogen Production from Solar Water-splitting

Alex Le Gal, Stéphane Abanades, Gilles Flamant, PROMES laboratory, CNRS, France

1 Introduction

Hydrogen is a promising energy carrier to replace fossil fuels that produce greenhouse gas and tend to decrease. However, it doesn't exist in the nature, thus it must be synthesized. Steam methane reforming along with electrolysis to a lower extent are currently the main used techniques to produce hydrogen but the former results in CO_2 emissions and the latter is limited by the energy efficiency. Thermochemical water splitting cycles are an alternative which use concentrated solar energy as the primary energy source. Direct water splitting needs a high temperature around 2500 K to allow dissociation and that's the reason why catalysts (reaction intermediates) are used. Mixed metal oxides are promising candidates for hydrogen production by solar thermochemical cycles. Such cycle consists of a two step process which implies a metallic oxide catalyst and water.

$$M_xO_y \rightarrow M_xO_{y-1} + ½\ O_2 \quad (1)$$

$$M_xO_{y-1} + H_2O \rightarrow M_xO_y + H_2 \quad (2)$$

During the first step, the oxide is thermally reduced by concentrated solar energy, which releases O_2 (1), then in the second step, the activated metallic oxide is hydrolyzed by steam, which produces H_2 (2).

There are many publications about such materials for this application. The cycle based on ZnO/Zn redox pair is investigated [1, 2] because it can theoretically produce a large amount of H_2/g (12,3mmol/g) during a single thermochemical cycle. But during the reduction step, the Zn produced is partially vaporized and partial recombination occurs during gas cooling, which requires a gas quench or a gas separation of Zn(g) and O_2 at high temperature to avoid recombination. The cycles with non volatile oxides thus appear as an attractive solution. Fe_3O_4/FeO cycle was first studied by Nakamura [3] and it presents a fairly good reactivity but the reduction temperature (1800K) is too high for current concentrated solar technologies and the reduced material is fused and sintered strongly, which decreases specific surface area and consequently material performance. To lower this activation temperature, the doping of magnetite with a metallic cation (Zn, Ni, Mn…) to form a ferrite is widely studied [4, 5, 6, 7, 8, 9]. Doped ferrites present a satisfactory theoretical production rate of H_2 (nearly 4.3 mmol/g depending on the metallic dopant) and a higher melting point than wustite induced by metal oxide properties. In this study, nickel ferrites were synthesized by different soft chemical routes such as coprecipitation of hydroxides, pechini process or hydrothermal treatment in view of enhanced thermal reduction yield. Then, the reactivity of the synthesized materials was investigated.

Abanades et al. [10] demonstrated that CeO_2/Ce_2O_3 cycle produces H_2 with a good reactivity of the Ce(III) species during hydrolysis (2,9 mmol/g), but the activation temperature is too high (2000°C) and there are mass losses induced by partial sublimation of ceria, which implies chemical efficiency decrease during cycling. Doping ceria with a metallic cation could reduce this activation temperature by inducing structural defects or oxygen vacancies [11, 12]. For the three-way catalysis application, Balducci et al. [13] showed that zirconium addition favors the reduction of ceria. Zirconium oxide can also contribute to avoid sintering thanks to the thermal properties of the oxide. In this study, the Zr-doped ceria was investigated targeting H_2 production. Ceria-based nano-materials are currently largely studied for their oxygen storage capacity or catalyst activity and thus, there are many researches about the synthesis of controllable morphology of this nanomaterial [14, 15, 16, 17]. Yuejuan [14] showed that using organic molecules as template agents for the preparation of high surface area and porous material improves catalytic activity. Yuan et al. [17] studied controlled synthesis to manipulate the shape, crystal plane and size of nano-materials in view of catalytic application and they demonstrated that better performing catalysts could be “designed” rather than prepared. In this paper, different synthesis methods of Zr-doped ceria were tested in view of enhanced reduction rate and hydrolysis reactivity. To conclude, the performances of nickel ferrite and Zr-doped ceria were compared in terms of H_2 production yield and cyclability.

2 Experimental

$NiFe_2O_4$ was synthesized by different wet chemical routes such as coprecipitation of hydroxides, pechini process, sol-gel or hydrothermal treatment to improve catalyst performance. These synthesis methods were initially chosen to obtain particular properties, typically powders with high surface area to favor kinetics and reduction rate during the first reduction step. Porous morphology with enhanced solid/gas interaction can also improve the hydrolysis yield. In a second part, zirconium-doped ceria ($Zr_xCe_{1-x}O_2$) was also synthesized by coprecipitation and the effect of a template agent (Cetyltrimethylammonium bromide) was studied targeting H_2 production improvement. X-ray diffraction analysis, SEM, BET and thermal gravimetric analysis were used to characterize the synthesized materials. Catalytic activity was investigated with a specific experimental device. The first step reduction was operated with a high temperature tubular furnace (1500°C max) which is equipped with an online O_2 trace analyzer (Zirconium oxide sensor). The powder was placed in an alumina crucible swept by an argon flow controlled with a mass flow-meter (200 $mL.min^{-1}$). The O_2 concentration was thus monitored continuously during the progress of the reduction reaction. The hydrolysis step was experimented in an other tubular furnace equipped with a catharometer for H_2 online measurement. A peristaltic pump was used to inject water which was vaporized inside the furnace and was transported by the carrier gas (argon).

3 Results

$NiFe_2O_4$ powders are well crystallized with cubic spinel structure and SEM images presented in figure 1 show three interesting morphologies. The powder synthesized by coprecipitation with surfactant PEG 400 (fig 1.a) is composed of spherical grains of 60 nm diameter and rods measuring some micrometers length and 200 nanometres width. The powder which was

synthesized by modified pechini process (fig 1.b) forms porous aggregates of about ten micrometers and non spherical grains appear relatively sintered. This porous morphology is explained by the fast degassing during the synthesis. The last image (fig 1.c) is representing $NiFe_2O_4$ synthesized by hydrothermal treatment; the material is composed of small spherical particles (60 nm diameter) without any sintering phenomenon. As it can be observed, the hydrothermal treatment avoids rod formation contrary to the synthesis without treatment. These three morphologies could enhance the reduction rate thanks to the porosity, the high surface area and good thermal properties.

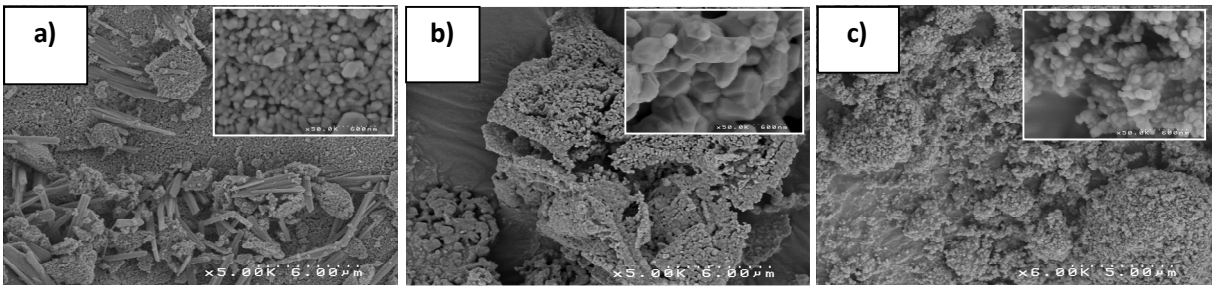

Figure 1: SEM images of $NiFe_2O_4$ synthesized by coprecipitation + PEG (a), modified pechini process (b) and with hydrothermal treatment (c).

The reduction step was investigated by thermal gravimetric analysis by heating a sample at 1400°C with a heating rate of 10°C/min and a dwell time of one hour. The mass loss associated to O_2 releasing begins at a temperature of about 1000°C for all the $NiFe_2O_4$ powders studied (fig. 2). The maximum reduction yield (Fe^{2+}/Fe^{3+}) of 19.2% is obtained for the powder synthesized by hydrothermal treatment but strong sintering of the powder decreases catalytic activity during the hydrolysis step. This reduction yield corresponds to 410 µmol of O_2 released per gram of material. The hydrolysis step was investigated using a tubular furnace and the H_2/O_2 ratio was calculated. Ideally, this ratio is equal to 2 but sintering phenomena reduce the hydrolysis yield, which implies reactivity losses during the cycle.

$Zr_xCe_{1-x}O_2$ was synthesized by coprecipitation of hydroxides with and without a template agent (CTABr). XRD patterns confirm that Zr-doped ceria samples are well crystallized with the CeO_2 cubic fluorite structure. FWHM of diffraction peaks of CTABr-synthesis are larger than for the powder synthesized without CTABr. The average crystallite sizes are calculated using the Scherrer's formula and are estimated around 7 nm and 17 nm, respectively. Surfactant effect thus allowed the synthesis of smaller particle size of doped-ceria. The reduction yield of CTABr-synthesized powder (Ce^{3+}/Ce^{4+}) measured by thermal gravimetric analysis is nearly three times higher than for the material synthesized by conventional coprecipitation (fig. 2). A reduction yield of 46% for CTABr-synthesized material corresponds to 565 µmol of O_2 released per gram.

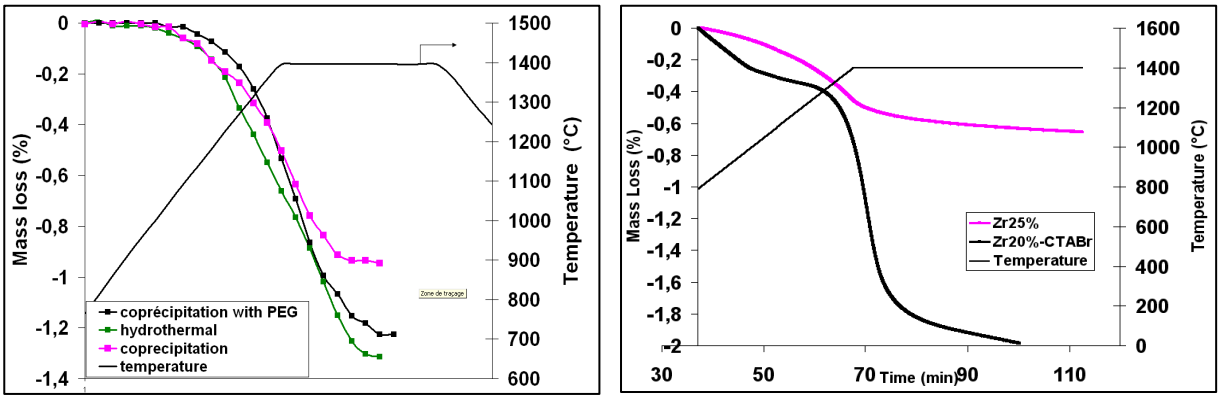

Figure 2: Thermal gravimetric analysis of $NiFe_2O_4$ (left) and Zr-doped ceria (right) synthesized by different methods.

After the reduction step, the CTABr-synthesized powder is strongly sintered, whereas the other material synthesized by coprecipitation still appears as a powder after the high temperature treatment. Consequently, the cycling was investigated with thermal gravimetric apparatus (fig. 3). First, the reduction step occurs by heating at 1400°C under argon flow, then the programmed temperature decreases to 1050°C and steam is introduced inside the furnace chamber with carrier gas (80%RH at 40°C) to react with the catalyst. This cycle was repeated twice to observe reactivity decrease. The Zr25% hydrolysis yield reached 83% and 89% during the first and the second hydrolysis reaction while it reached 18% and 22% for Zr20%-CTABr. The yield of the first hydrolysis reaction corresponds to 335 µmol of H_2 produced per gram of 25%Zr and 213 µmol of H_2 produced per gram of Zr20%-CTABr. The H_2/O_2 ratio, ideally equal to 2, which is a good indicator of materials cyclability is equal to 1.8 for Zr25%, which means that no significant reactivity losses happened during the cycle.

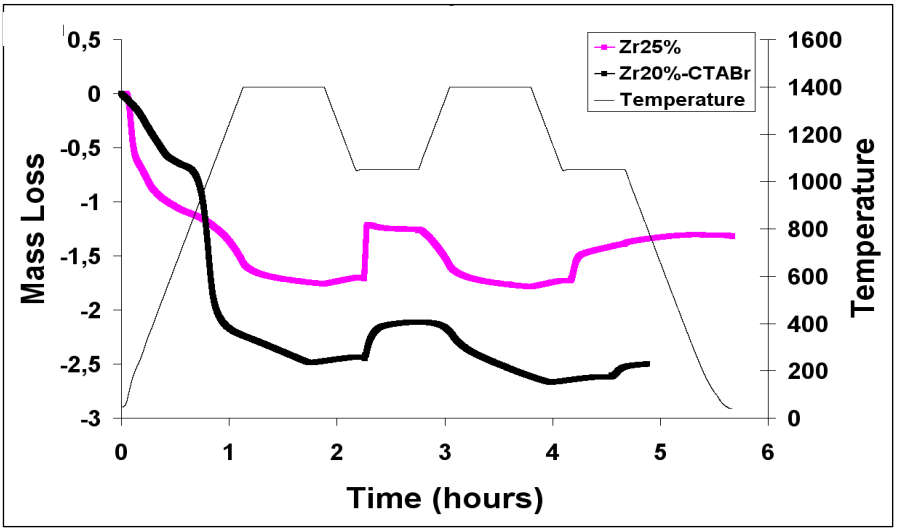

Figure 3: Thermal gravimetric analysis of water splitting cycle with $Zr0_{.25}Ce_{0.75}O_2$ synthesized by coprecipitation and $Zr_{0.2}Ce_{0.8}O_2$ synthesized with CTABr.

4 Conclusion

$NiFe_2O_4$ and Zr-doped ceria were synthesized by different soft chemical routes to improve thermal reduction rate. The highest reduction yield reached with a nickel ferrite was 19.2% (Fe^{2+}/Fe^{3+}) corresponding to 410 µmol O_2/g, while the highest yield with Zr-doped ceria was 46% corresponding to 565 µmol O_2/g. Both materials showed strong sintering after the reduction step, which implies reactivity losses during cycling. The synthesis methods did not avoid sintering for $NiFe_2O_4$ but concerning Zr-doped ceria, coprecipitation method without CTABr alleviated sintering and allowed the material cycling without reactivity loss. During cycling, the catalyst produced about 335 µmol of H_2 per gram with a H_2/O_2 ratio nearly approaching 2. This study demonstrated that Zr-doped ceria is a promising material because the reduction temperature is below 1500°C and no significant reactivity losses are observed during cycling.

References

[1] Steinfeld A. (2002) Solar hydrogen production via a two-step water-splitting thermochemical cycle based on Zn/ZnO redox reactions. Int J Hydrogen Energy [27] p 611-619

[2] Weidenkaff A., Reller A., Wokaun A., and Steinfeld A. (2000) Thermogravimetric analysis of the ZnO/Zn water splitting cycle, Thermochemical Acta [359] p 69-75

[3] Nakamura T. (1977) Hydrogen production from water utilizing solar heat at high temperature, Solar Energy, [19] p467-475

[4] Tamaura Y., Steinfeld A., Kuhn P., Seberger K. (1995) Production of solar hydrogen by a 2-step, water splitting thermochemical cycle, Energy [20] p325-330

[5] Tamaura Y., Kojima M., Sano T., Ueda Y., Hasegawa N., Tsuji M. (1998) Thermodynamic evaluation of water splitting by a cation excessive(Ni,Mn) ferrite, International Journal of Hydrogen Energy [23] p1185-1191

[6] Han S. B., Kang T. B., Joo O. S., Jung K. D. (2007) Water splitting for hydrogen production with ferrites, Solar Energy, [81] p 623-628

[7] Kaneko H., Yokoyama T., Fuse A., Ishihara N., Tamaura Y. (2006) Synthesis of new ferrite, Al-Cu ferrite, and its oxygen deficiency for solar H_2 generation from H_2O, International journal of hydrogen energy [31] p 2256-2265

[8] Kodama T., Gokon N., Yamamoto R., (2008) Thermochemical two-step water splitting by ZrO2-supported NixFe3-xO4 for solar hydrogen production, Solar Energy [82] p 73-79

[9] Gokon N., Muramyama H., Nagasaki A., Kodama T. (2009) Thermochemical two-step water splitting cycles by monoclinic ZrO2-supported $NiFe_2O_4$ and Fe_3O_4 powders and ceramic foam devices, Solar Energy [83] p 527-537

[10] Abanades S., Flamant G. (2006) Thermochemical hydrogen production from a two-step solar-driven water-splitting cycle based on cerium oxides, Solar Energy [80] p 1611-1623

[11] Kaneko H., Miura T., Ishihara H., Taku S., Yokoyama T., Nakajima H., Tamaura Y. (2007) Reactive ceramics of CeO_2-MO_x (M = Mn, Fe, Ni, Cu) for H_2 generation by two-step water splitting using concentrated solar thermal energy, Energy [32] p 656-663

[12] Kaneko H., Ishihara H., Taku S. (2008) Cerium ion redox system in CeO2-xFe2O3 solid solution at high temperature in the two-step water-splitting reaction for H2 generation, Journal of Materials Science [43] p 3153-3161

[13] Balducci G., Kašpar J., Fornasiero P., Graziani M., Islam M.S., Gale J.D. (1997) Computer simulation studies of bulk reduction and oxygen migration in CeO_2-ZrO_2 solid solutions. J Phys Chem B [101] p 1750-1753

[14] Yuejuan W., Jingmeng M., Mengfei L., Ping F., Mai H. (2007) Preparation of high surface area nano-CeO2 by template-assisted precipitation method, Journal of Rare Earth [25] p 58-62

[15] Feng R., Yang X., Ji W., Au C. T. (2008) Hydrothermal synthesis of stable mesoporous ZrO2-Y2O3 and CeO2-ZrO2-Y2O3 from simple organic salts and CTAB template in aqueous medium, Materials Chemistry and Physics [107] p 132-136

[16] Pan C., Zhang D., Shi L. (2008) CTAB assisted hydrothermal synthesis ,controlled conversion and CO oxidation properties of CeO2 nanoplates, nanotubes, and nanorods, Journal of solid state chemistry [181] p 1298-1306

[17] Yuan Q., Duan H., Li L., Sun L.D., Zhang Y., Yan C.H. (2009) Controlled synthesis and assembly of ceria-based nanomaterials, Journal of colloid and interface science [335] p 151-167